POLISH ARCHIVES OF
Internal Medicine
POLSKIE ARCHIWUM MEDYCYNY WEWNĘTRZNEJ

ONLINE FIRST

This is a provisional PDF only. Copyedited and fully formatted version will be made available soon.

Radiomic virtual biopsy for phenotyping of abnormal cardiac masses based on computed tomography: proof of concept study

Authors: Piotr Trochimiuk, Agnieszka Segiet-Święcicka, Mariusz Kruk, Edyta Kaczmarska-Dyrda, Zofia Dzielińska, Marcin Demkow, Cezary Kępka

Article type: Original article

Received: June 5, 2026.

Revision accepted: July 3, 2026.

Published online: July 9, 2026.

ISSN: 1897-9483

Pol Arch Intern Med.

doi:10.20452/pamw.17346

Radiomic virtual biopsy for phenotyping of abnormal cardiac masses based on computed tomography: proof of concept study

Piotr Trochimiuk[1], Agnieszka Segiet-Święcicka[2], Mariusz Kruk[3], Edyta Kaczmarska-Dyrda[1], Zofia Dzielińska[1], Marcin Demkow[1], Cezary Kępka[1]

[1] Department of Coronary and Structural Heart Diseases, National Institute of Cardiology Stefan Cardinal Wyszyński – National Research Institute, Warszawa, Poland

[2] Department of Coronary Artery Disease and Cardiac Rehabilitation, National Institute of Cardiology Stefan Cardinal Wyszyński – National Research Institute, Warszawa, Poland

[3]Admissions and Emergency Diagnostics Department, National Institute of Cardiology Stefan Cardinal Wyszyński – National Research Institute, Warszawa, Poland

Correspondence to: Piotr Trochimiuk, MD, Department of Coronary and Structural Heart Diseases, National Institute of Cardiology Stefan Cardinal Wyszyński – National Research Institute, ul. Alpejska 42, 04-628 Warszawa, Poland, phone: +48 693899600, email: ptrochimiuk@ikard.pl

Supplementary material: Supplementary material is available at www.mp.pl/paim.

Keywords: cardiac masses, computed tomography, myxoma, radiomics, thrombus, virtual biopsy

Abstract

Introduction: Cardiac masses can present a diagnostic challenge on cardiac imaging. Differentiating between tumors such as myxomas and non-neoplastic lesions like thrombi is essential for appropriate management and treatment planning.

Objectives: The aim of this study was to explore the feasibility of radiomics-based "virtual biopsy" in distinguishing between different types of cardiac masses on computed tomography (CT).

Patients and methods: 89 patients were included in the analysis. 42 (47.2%) were diagnosed with myxoma, 37 (41.6%) were diagnosed with thrombus and 10 (11.2%) had other diagnoses [fibroelastoma in 6 (6.7%) cases, sarcoma in 2 (2.2%) cases, angioma and metastasis in one (1.1%) case each]. The ROI selection, and calculation of the radiomic features was done with syngo.via Frontier Radiomics. 3D ROI of the cardiac masses for CT examination has been manually delineated. A multivariate LASSO-based model was developed for both binary (thrombus vs. tumor) and multiclass (thrombus vs. myxoma vs. other) classification.

Results: The exploratory multiclass radiomics model demonstrated preliminary discriminatory performance, with validation AUCs ranging from 77.1% to 93.3%; however, class-specific estimates, particularly for the heterogeneous "other" category, should be interpreted with caution due to the small validation cohort. These findings suggest that radiomics features can capture subtle differences between distinct cardiac mass types, enabling noninvasive tissue characterization.

Conclusion: This proof-of-concept study provides the first evidence that a multiclass CT-based radiomics model can differentiate between myxomas, thrombi, and other cardiac masses. Radiomics-based "virtual biopsy" may potentially complement conventional imaging; however, these exploratory findings require validation in larger, multicentre cohorts before clinical application.

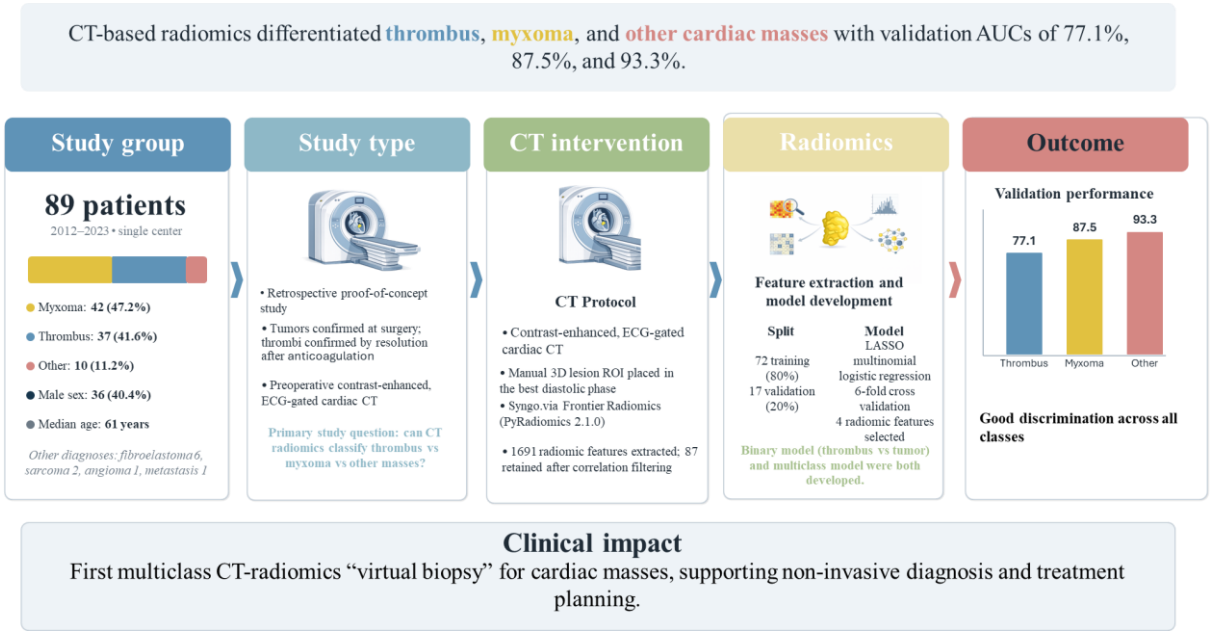

Introduction

Cardiac masses represent a heterogeneous group of lesions that can be either tumors (primary/metastatic, malignant/benign) or non-neoplastic such as thrombus, vegetations, calcifications and etc. [1, 2]. Clinical presentation ranges from incidental discovery on imaging tests ordered for other reasons to life-threatening presentations such as cardiac tamponade, arrhythmia, obstruction, and systemic embolization [2] The symptoms depend on tumor size, site and the extent of infiltration into the neighboring tissue [3]. The most observed non-neoplastic change found in studies is the presence of thrombus. Among neoplastic conditions, myxomas are the most prevalent, followed by metastases, while primary malignant heart tumors are relatively rare. Further prognosis, management and its urgency critically depend on the histopathological diagnosis, which comprises a gold standard (6). Current non-invasive diagnostics in most cases lacks adequate sensitivity and specificity to provide the precise tumor diagnosis. Despite the few reports [4-8], preoperative catheterization with endomyocardial biopsy of tumors confined to the right heart is rarely performed due to the technical difficulties and high risk of procedure [2]. A presumptive diagnosis is typically made on medical history

and by using multimodality non-invasive imaging techniques. Echocardiography, computed tomography or magnetic resonance enable an accurate assessment of anatomic location, size and functional implications but only poor tissue characterization. In many cases a definitive diagnosis requires surgical intervention.

Radiomics based extraction of features from medical images using advanced mathematic algorithms allows to characterize pathologies beyond what can be observed by the radiologist's "naked" eye. Radiomics analysis may be used to characterize cardiac masses to achieve tissue characterization as a "virtual biopsy". Recently, radiomics was proven to differentiate between cardiac tumors versus thrombi [9].

The aim of this study is to evaluate the ability of radiomic analysis to further differentiate between cardiac masses, in particular differentiate between a relatively frequent and benign tumor - myxoma versus others.

Despite advances in multimodality imaging, the noninvasive classification of cardiac masses continues to pose a formidable clinical challenge. The vast majority of available studies have focused on binary separation of thrombus versus tumor, with limited insight into the phenotypic diversity of individual tumor subtypes. Yet in daily clinical practice, the cardiologist and cardiac surgeon are confronted not only with the distinction between thrombus and neoplasm, but also with the need to differentiate myxomas from other benign and malignant tumors, each carrying distinct therapeutic implications. To our knowledge, no previous investigation has systematically evaluated a multiclass CT-based radiomics model encompassing myxomas, thrombi, and additional tumor types within a single analytic framework. We therefore designed this proof-of-concept study to explore whether radiomics can provide such a granular classification, thereby extending the concept of a "virtual biopsy" toward more clinically relevant decision-making.

Patients and methods

Study population

The study group consisted of patients hospitalized in the National Institute of Cardiology, Warsaw, Poland between years 2012–2023.

Inclusion criteria were:

1. Patients undergoing cardiac surgery for a cardiac mass, with available preoperative cardiac CT and histopathological confirmation of the lesion.
2. Patients with a cardiac mass suggestive of thrombus on CT at typical locations (left atrial appendage or left ventricular apex), with documented complete resolution after anticoagulation therapy.

Exclusion criteria were:

1. Inadequate CT image quality, defined as severe motion artifacts, insufficient contrast opacification, excessive image noise, or incomplete visualization of the lesion precluding reliable segmentation and radiomics analysis.

2. Incomplete clinical or imaging data, or lack of definitive diagnostic confirmation.

Of 79 patients who underwent cardiac surgery due cardiac masses with pre-surgery cardiac CT and histopathological tumor analysis, 27 were excluded due to unsatisfactory CT image quality totaling in 52 patients. 37 consecutive patients with a cardiac mass suggestive of thrombus in cardiac CT at typical localization of massed with documented follow up of remission after anticoagulation therapy.

For surgically treated tumors, the reference standard was histopathological diagnosis. For thrombus cases, the reference standard was based on characteristic CT appearance at typical locations and documented complete resolution after anticoagulation therapy.

A detailed overview of patient identification, exclusion criteria, reference standards, and final cohort composition is presented in Figure 1.

CT protocol and analysis.

The CT examinations were performed on SOMATOM Force (Siemens Healthcare, Erlangen, Germany) and SOMATOM Definition Flash (Siemens Healthcare, Erlangen, Germany) with a gated cardiac protocol with contrast agent. Patients without contraindications received intravenous metoprolol (2.5 mg boluses titrated up to 10 mg) to limit heart rate below 65 beats/min, and sublingual nitroglycerin was administered prior to image acquisition on a regular basis. The contrast transit time was estimated by injection of a test bolus. For acquisition of the volume dataset, 60 to 120 ml iodinated contrast material (Iomeron 400, Bracco Altana Pharma, Konstanz, Germany) was injected intravenously at a rate of 6 ml/s (Definition Flash) or 4.5 ml/s (Force). Data were acquired using a retrospectively electrocardiogram-gated or prospectively electrocardiogram-triggered protocol with a beam collimation, 128 × 0.6-mm (Definiton Flash) or 192 × 0.6-mm (Force) and tube voltage of 70– 120 kV adjusted to body mass index. Radiation dose reduction strategies including electrocardiogram-gated tube current modulation and prospective axial triggering were used whenever feasible. The best diastolic phases were selected for the placement of region of interest (ROI).

The ROI selection, calculation of the radiomic features was done with syngo.via Frontier Radiomics research prototype version 1.2.5 (Siemens Healthcare, Erlangen, Germany). This prototype is an implementation of radiomic framework “PyRadiomics” version 2.1.0. No additional intensity normalization or voxel-size resampling was performed before radiomic feature extraction. Gray-level discretization and feature calculation were performed according to the default settings of the software implementation. Anatomical lesion location was not explicitly included as a model feature. The examinations were acquired using two CT scanner platforms from the same vendor and comparable cardiac CT acquisition protocols.

Region was drawn using 3D tools implemented in Frontier Radiomics prototype. Total number of features extracted from the objects was 1691. 1Shape-related features were deliberately excluded from the analysis, as conservative ROI placement and indistinct lesion borders could bias geometric measurements. Instead, the analysis prioritized intensity- and texture-based descriptors, including wavelet-transformed first-order statistics, which can indirectly capture morphological and heterogeneity differences.

Statistical analysis

Demographic data were presented using descriptive statistics, absolute and relative frequency was reported for categorical variables and mean with standard deviation, median with first and third quartile and minimum and maximum values were reported for continuous variables. Aim of the analysis was to assess the predictive properties of the radiomic features in differentiation between cardiac masses classified as thrombus, myxoma, or other. To achieve the analysis aims, binary classification model for diagnosis of thrombus vs. other and multiclass classification model for diagnosis of thrombus vs. myxoma. vs other was built.

Prior to feature selection and model building, no data standardization or transformation was conducted. To reduce dimensionality and limit redundancy, strongly correlated radiomic predictors were removed using a Spearman correlation coefficient threshold of ≥ 0.6, which reduced the feature space from 1691 to 87 predictors. LASSO regression was subsequently applied as an embedded feature-selection and regularization method. Model parameters were selected using cross-validation within the training dataset. Analysis set was divided to training dataset (80% of observations, n = 72 subjects) and validation dataset (20% of observations, n = 17 subjects). The LASSO (least absolute shrinkage and selection operator) logistic regression was applied for feature selection and binary classification model building for thrombus vs. other classification. A 7-fold cross validation with maximalization of area under the curve (AUC) of the receiver operating characteristic (ROC) was applied in order to select model parameters.

The LASSO multinomial logistic regression, with 6-fold cross validation and minimization of misclassification error, was applied for feature selection and multiclass classification model building for thrombus vs. myxoma vs. other classification. Binary classification models performance on training and validation datasets was assessed using ROC curves analysis and model calibration. AUC for ROC curve with 95% confidence interval (CI), specificity, sensitivity, and accuracy at optimal cut-off (defined as a predicted probability value that minimizes ROC curve distance to the point of 100% sensitivity and 100% specificity), as well as plot of ROC curve were reported. Calibration plots (probability of thrombus diagnosis predicted in model vs observed) were presented. In assessment of multiclass classification models performance, accuracy (overall and one-class-vs-rest), precision (one-class-vs-rest), and AUC for ROC curve with 95% CI (one-class-vs-rest) on training and validation datasets were reported. Level of statistical significance was set at 0.05. All statistical analyses were performed using R statistical software, version 4.1.3 (R Foundation for Statistical Computing, Vienna, Austria). The packages 'glmnet' and 'rpart' were used for model building.

Results

Baseline characteristics

A total number of n = 89 patients were included in the analysis. Out of them, 42 (47.2%) were diagnosed with myxoma, 37 (41.6%) were diagnosed with thrombus and 10 (11.2%) had other diagnoses (fibroelastoma in 6 (6.7%) cases, sarcoma in 2 (2.2%) cases, angioma and metastasis in one (1.1%) case each). The median of age on the examination day of patients included in the analysis was 61.0 (IRQ 50.0–69.0), range 23–86 years; 36 (40.4%) patients were male. Proportion of males was higher for thrombus (56.8%) than for myxoma (28.6%) or other diagnoses (30.0%) (P = 0.034). Age did not differ significantly between the subgroups by diagnosis. The median of object volume was 3.52 (IQR 1.12–9.70) ml, and median of object

maximal diameter was 30.12 (IQR 19.60–40.00) mm, and for both measurements object size was significantly larger for myxoma than for thrombus or other diagnoses ($P = 0.001$ and $P = 0.034$ respectively) (Table 1).

Models for differentiation between cardiac masses based on radiomic features

Feature selection and model building was performed on a subset of radiomic features after removal of strongly correlated predictors, which resulted in reduction of feature space dimensionality from 1691 to 87 predictors. LASSO regression method was used to construct binary classification model for diagnosis of thrombus vs. other (presented in appendix 1) and multiclass classification model for diagnosis of thrombus vs. myxoma vs. other diagnoses based on the radiomic features. Multiclass classification models for diagnosis of thrombus vs. myxoma vs. other diagnoses fitted using a LASSO multinomial regression was based on a total of 4 features (Table 2), out of which three were also included in binary classification model. Detailed model coefficients are provided in Supplementary material, *Table S1*. Fitted classification model demonstrated encouraging but preliminary discriminatory performance on both training and validation datasets, with AUC values ranging from 79.9% to 90.2% for one-versus-rest analyses in the training cohort and from 77.1% to 93.3% in the validation cohort (Table 3, Figure 2A-C, Table 4). Class-specific performance for the "other" category should be interpreted with particular caution. In the validation cohort, no "other" cases were correctly classified, and the reported one-vs-rest accuracy was mainly driven by specificity due to class imbalance rather than by correct identification of this subgroup.

Discussion

The findings of the present study should be interpreted within the context of an exploratory proof-of-concept design. Although the models demonstrated preliminary discriminatory performance, the limited sample size, particularly for rare tumor subtypes grouped within the

"other" category, substantially restricts the stability and generalizability of the results. Therefore, the present analysis should be considered hypothesis-generating rather than confirmatory.

Our multiclass classification model using LASSO multinomial regression demonstrated encouraging but preliminary discriminatory performance, with AUCs ranging from 77.1% to 93.3% in the validation dataset. These results suggest that radiomics features can capture the subtle differences between various types of cardiac masses, enabling a more granular classification. The radiomic features selected by the LASSO-based models provide insights into the key characteristics that differentiate cardiac masses. Although shape-related features were deliberately excluded due to segmentation constraints, the binary classification model retained texture- and wavelet-transformed intensity features. These descriptors likely capture morphological and heterogeneity differences indirectly, suggesting that radiomics can provide surrogate markers of lesion shape and composition even without explicit geometric measurements. Similarly, the multiclass model incorporated features from different categories, indicating that a combination of texture- and intensity-based descriptors is necessary for a more refined classification of cardiac masses.

Although these findings suggest potential future clinical applicability, the present results are insufficient to support changes in clinical decision-making and require validation in larger multicenter cohorts. The "other" category included biologically heterogeneous lesions with distinct pathological backgrounds and imaging characteristics, including fibroelastoma, sarcoma, angioma, and metastasis. These lesions were grouped together because individual tumor subtypes were too rare for separate modelling. Consequently, analyses involving this subgroup should be considered exploratory rather than confirmatory, and the reported performance metrics should be interpreted with caution.

Radiomics has been extensively applied across various cancer types, including lung cancer, breast cancer, genitourinary cancers, digestive system cancers, and brain tumors.[10] However, its use within cardio-oncology remains limited. Only a single previous study referring to cardiac mases showed ability of radiomics models to differentiate between cardiac tumors and thrombi, achieving an AUC of 0.973 [9].

While promising, that study did not address distinctions among specific non-thrombotic tumor types. In contrast, our current research employs a multiclass classification model capable of differentiating not only between thrombus and tumor, but also among various cardiac masses, thereby more closely reflecting the diversity encountered in clinical practice.

The present study did not include a direct comparison with expert reader assessment or with models based on simple clinical and CT descriptors such as lesion size, location, or morphology. Therefore, the incremental diagnostic value of radiomics over conventional imaging assessment remains unproven.

Conclusions

This exploratory proof-of-concept study suggests that CT-based radiomics may enable preliminary differentiation between thrombi, myxomas, and other cardiac masses. However, the findings should be interpreted cautiously due to the limited sample size, class imbalance, heterogeneous “other” category, and lack of external validation. Further multicenter studies with larger cohorts, harmonized acquisition protocols, reproducibility assessment, and independent validation are required before potential clinical application.

Limitations

Several important limitations should be acknowledged. First, this was an exploratory proof-of-concept study with a relatively small sample size. Although the cohort included myxomas, thrombi, and other cardiac masses, the number of rare tumor subtypes was limited. In particular, the “other” category consisted of biologically heterogeneous lesions, including fibroelastoma,

sarcoma, angioma, and metastasis. Because individual tumor types were too infrequent for separate modelling, analyses involving this subgroup should be considered exploratory rather than confirmatory.

Second, different reference standards were used across diagnostic groups. Histopathology served as the reference standard for surgically treated tumors, whereas thrombus diagnosis was based on characteristic CT appearance and complete resolution after anticoagulation therapy. This approach may have introduced verification bias and may have favored inclusion of treatment-responsive thrombi, while chronic or organized thrombi that can mimic neoplastic lesions were likely underrepresented.

Third, although anatomical lesion location was not explicitly included as a model feature, indirect location-related imaging characteristics may still have influenced radiomics signatures. This is particularly relevant for thrombi, which were typically located in the left atrial appendage or left ventricular apex.

Fourth, segmentation was performed by a single reader, and no intra-observer or inter-observer reproducibility assessment was conducted. Therefore, the robustness of radiomics features with respect to segmentation variability could not be evaluated.

Fifth, although correlation filtering, LASSO regularization, and cross-validation were used to reduce dimensionality and limit overfitting, the high feature-to-sample ratio remains an important limitation. Therefore, the selected radiomic features and model coefficients should be considered potentially unstable and sample dependent. Furthermore, because feature selection was performed in a relatively small dataset with a high feature-to-sample ratio, the specific radiomic features retained in the final model should be regarded as potentially unstable and sample-dependent. Consequently, the findings should be interpreted as hypothesis-generating rather than evidence of definitive feature importance.

Sixth, the validation strategy was based on a single internal train–validation split, with a relatively small validation cohort and no external validation. Consequently, the reported performance estimates may be unstable and potentially optimistic, particularly for the heterogeneous “other” category.

Seventh, the study did not include direct comparison with expert reader assessment or with models based on simple clinical and CT descriptors such as lesion size, location, or morphology. Therefore, the incremental diagnostic value of radiomics over conventional imaging assessment remains unproven.

Finally, the single-center design and relatively consistent CT acquisition protocol may have improved internal consistency but limit generalizability to other institutions, scanner vendors, reconstruction algorithms, and acquisition protocols. Larger multicenter studies with standardized imaging protocols, reproducibility assessment, and external validation are needed before potential clinical implementation.

Despite these limitations, the study provides unique, preliminary evidence supporting the feasibility of CT-based multiclass radiomics for characterization of cardiac masses, and provides the most robust material for such analysis.

Article information

Acknowledgments: None

Funding: This research received no external funding. No financial support was provided by any organization for the conduct of this study.

Contribution statement: PT.: data collection, image analysis, interpretation of data, drafting of the manuscript. A S-Ś: statistical analysis; MK conceptualization, study design, supervision; EK-D: data collection, ZD data critical revision of the manuscript. MD: critical revision of the

manuscript. CK: final approval of the manuscript. All authors have read and approved the final version of the manuscript.

AI statement: Artificial intelligence was not used in preparation of this manuscript

How to cite: Trochimiuk P, Segiet-Święcicka A, Kruk M, et al. Radiomic virtual biopsy for phenotyping of abnormal cardiac masses based on computed tomography: proof of concept study. Pol Arch Intern Med. 2026; XX: 17346. doi:10.20452/pamw.17346

References

1. Bussani R, Castrichini M, Restivo L, et al. Cardiac tumors: diagnosis, prognosis, and treatment. Curr Cardiol Rep. 2020; 22: 169.
2. Poterucha TJ, Kochav J, O'Connor DS, et al. Cardiac tumors: clinical presentation, diagnosis, and management. Curr Treat Options Oncol. 2019; 20: 66.
3. Hoffmeier A, Sindermann JR, Scheld HH, Martens S. Cardiac tumors—diagnosis and surgical treatment. Dtsch Arztebl Int. 2014; 111: 205-211.
4. Ionescu D, Stone D, Stone J, et al. The role of endomyocardial biopsy in cardiac tumors diagnosis. J Clin Oncol. 2017; 35: e22536.
5. Zanobini M, Dello Russo A, Saccocci M, et al. Endomyocardial biopsy guided by intracardiac echocardiography as a key step in intracardiac mass diagnosis. BMC Cardiovasc Disord. 2018; 18: 15.
6. Mitchell AR, Timperley J, Hudsmith L, et al. Intracardiac echocardiography to guide myocardial biopsy of a primary cardiac tumour. Eur J Echocardiogr. 2007; 8: 505-506.

7. Segar DS, Bourdillon PD, Elsner G, et al. Intracardiac echocardiography-guided biopsy of intracardiac masses. J Am Soc Echocardiogr. 1995; 8: 927-929.
8. Park KI, Kim MJ, Oh JK, et al. Intracardiac echocardiography to guide biopsy for two cases of intracardiac masses. Korean Circ J. 2015; 45: 165-168.
9. Lee JW, Park CH, Im DJ, et al. CT-based radiomics signature for differentiation between cardiac tumors and thrombi: a retrospective, multicenter study. Sci Rep. 2022; 12: 8173.
10. Li S, Zhou B. A review of radiomics and genomics applications in cancers: the way towards precision medicine. Radiat Oncol. 2022; 17: 217.

Table 1 Demographics and computed tomography measurements summary at baseline.

Characteristic		**Overall, N = 89**	**Myxoma, N = 42**	**Thrombus, N = 37**	**Other, N = 10**	***P* value**
Gender, n (%)	Male	36 (40.4)	12 (28.6)	21 (56.8)	3 (30.0)	0.034
	Female	53 (59.6)	30 (71.4)	16 (43.2)	7 (70.0)	
Age, years						
Median, IQR		61.0 (50.0–69.0)	59.0 (50.0–65.8)	64.0 (48.0–70.0)	65.0 (58.5–71.5)	0.560
Range		23–86	38–80	23– 86	27–78	
Object volume, ml						
Median, IQR		3.52 (1.12–9.70)	7.03 (2.63–12.21)	1.40 (1.02–4.40)	0.83 (0.39–15.62)	0.001

Range	0.2–243.2	0.6–70.3	0.4– 51.0	0.2– 243.2	
Object maximal diameter, mm					
Median, IQR	30.12 (19.60– 40.00)	32.79 (22.97– 43.29)	26.10 (18.78– 34.71)	14.90 (12.96– 40.27)	0.034
Range	9.1–104.5	15.5–69.3	14.2–96.1	9.1– 104.5	
Abbreviations: IQR, interquartile range					

Table 2 Categories of radiomic features retained in the final multiclass LASSO model

Feature category	**Selected feature**	**Image transformation**
Texture (GLRLM)	ShortRunLowGrayLevelEmphasis	Exponential
First-order intensity	Minimum	Square
First-order intensity	Skewness	Wavelet HLL
First-order intensity	Skewness	Wavelet LLH

Detailed model coefficients are provided in Supplementary material, *Table S1*.

Abbreviations: GLRLM, Gray-level run length matrix

Table 3 Discrimination performance of multiclass classification model for diagnosis of thrombus vs. myxoma vs. other diagnoses fitted using LASSO logistic regression

Dataset	**Classification type**	**AUC, %**	**AUC 95% CI, %**	**Accuracy, %**	**Precision, %**
Training, n = 72	Overall (3-class)	-	-	73.6	-
	Thrombus vs. rest	90.2	83.3–97.0	77.8	78.3
	Myxoma vs. rest	89.9	82.5–97.4	76.4	86.2
	Other vs. rest	79.9	60.3–99.5	93.1	92.8
Validation, n = 17	Overall (3-class)	-	-	70.6	-
	Thrombus vs. rest	77.1	52.8–100.0	70.6	77.8
	Myxoma vs. rest	87.5	70.4–100.0	82.4	87.5
	Other vs. rest	93.3	80.3–100.0	88.2	88.2

Abbreviations: AUC, area under the curve

Table 4 LASSO model– contingency table for predicted vs observed, training dataset (n = 72) and test dataset (n = 17)				
Dataset	Predicted:	Observed: myxoma	Observed: other	Observed: thrombus
Training (n = 72)	myxoma	30 (41.7%)	3 (4.2%)	10 (13.9%)
	other	0 (0.0%)	3 (4.2%)	0 (0.0%)
	thrombus	4 (5.6%)	2 (2.8%)	20 (27.8%)
Test (n = 17)	myxoma	7 (41.2%)	0 (0.0%)	2 (11.8%)
	other	0 (0.0%)	0 (0.0%)	0 (0.0%)
	thrombus	1 (5.9%)	2 (11.8%)	5 (29.4%)

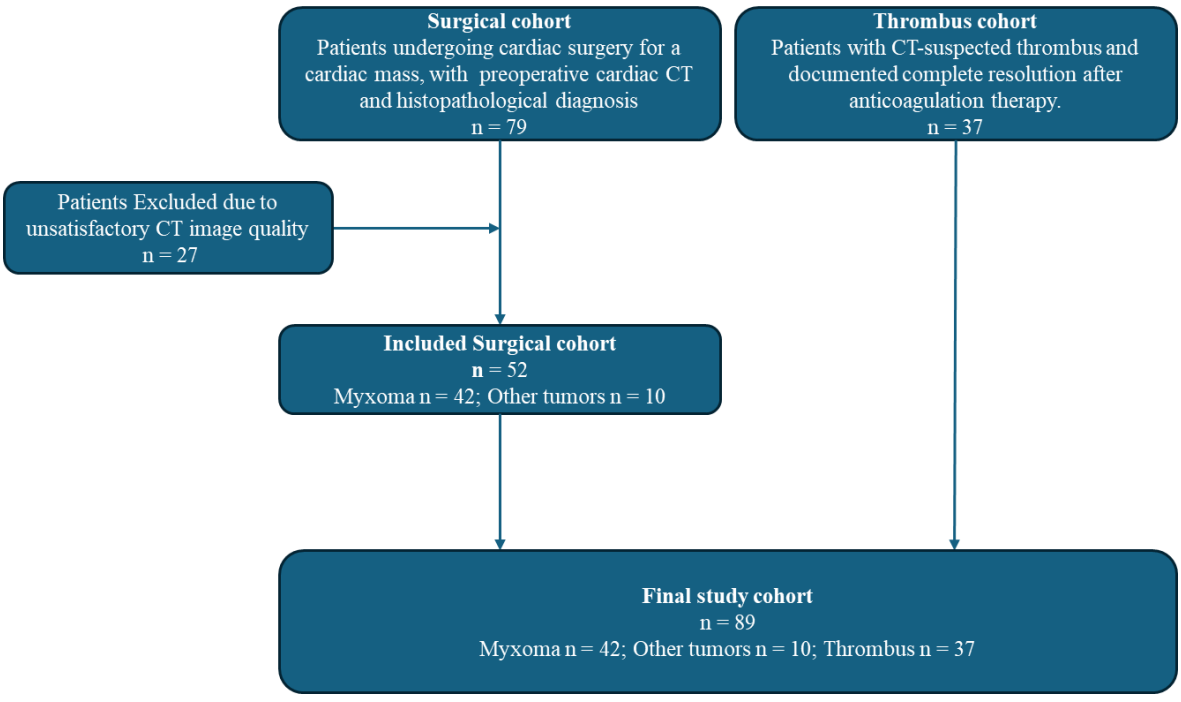

Figure 1 Study flowchart showing patient selection, exclusion criteria, and final diagnostic groups included in the radiomics analysis.

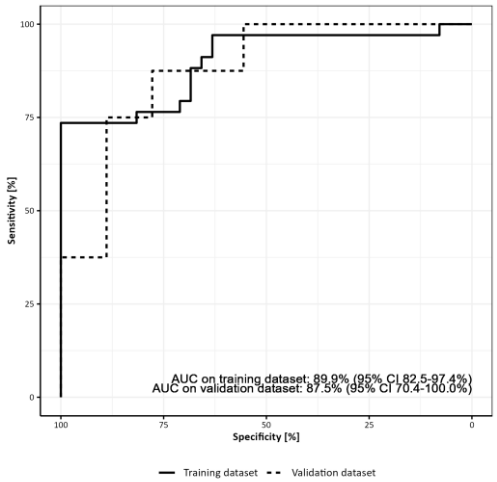

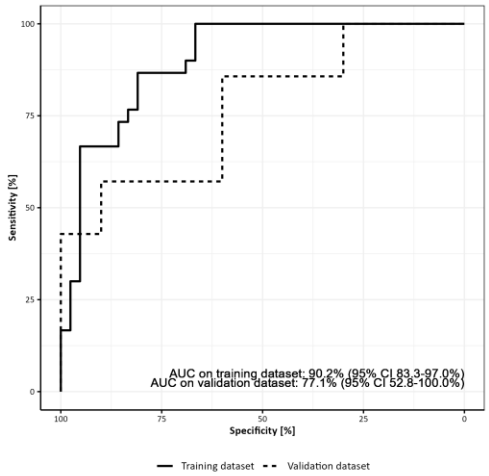

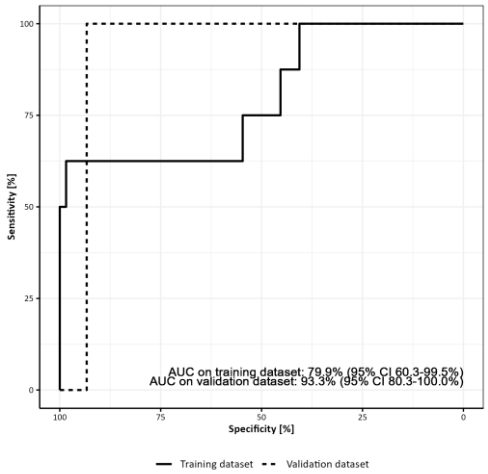

Figure 2 A – ROC curve of multiclass classification model for diagnosis myxoma vs others (thrombus or other) fitted using LASSO logistic regression; **B** – ROC curve of multiclass classification model for diagnosis thrombus vs others (myxoma or other) fitted using LASSO logistic regression; **C** – ROC curve of multiclass classification model for diagnosis other vs thrombus or myxoma fitted using LASSO logistic regression

Short title: Radiomic virtual biopsy for phenotyping of abnormal cardiac masses based on CT